Journal of Food Bioactives
International Society for Nutraceuticals and Functional Foods
Original Research
J. Food Bioact. 2026;33:63–72

Bioactive-rich kale extracts protect against UV-induced oxidative stress and DNA damage in human skin fibroblasts

Harichandana Valisakkagari[a] and H.P. Vasantha Rupasinghe[a,b*]

[a]Department of Plant, Food, and Environmental Sciences, Faculty of Agriculture
Dalhousie University, Truro, Nova Scotia, Canada
[b]Department of Pathology, Faculty of Medicine, Dalhousie University, Halifax, Nova Scotia, Canada
[*]**Corresponding author:** H.P. Vasantha Rupasinghe, Department of Plant, Food, and Environmental Sciences, Faculty of Agriculture, Dalhousie University, Truro, Nova Scotia, Canada. Tele: +1 (902)-893-6623; E-mail: vrupasinghe@dal.ca
DOI: 10.26599/JFB.2026.95033440
Received: October 22, 2025; **Revised received & accepted:** December 01, 2025
Citation: Valisakkagari, H., and Rupasinghe, H.P.V. (2026). Bioactive-rich kale extracts protect against UV-induced oxidative stress and DNA damage in human skin fibroblasts. J. Food Bioact. 33: 63–72.

Abstract

Exposure to ultraviolet (UV) radiation causes oxidative stress and DNA damage in skin cells. This study investigated the protective effects of bioactive-rich extracts prepared from upcycled kale powder using UV-induced human skin fibroblasts (WS1 cells) *in vitro*. The extracts were prepared using ultrasound-assisted extraction [K(U)] and microwave-assisted extraction [K(M)]. The Fourier transform infrared spectroscopy (FT-IR) and ultra-high-performance liquid chromatography electrospray ionization mass spectrometry (UPLC-ESI-MS) demonstrated that K(M) contains higher concentrations of major bioactive phytochemicals, including phenolic acids, carotenoids, glucosinolates and flavonoids, than K(U). Both extracts contributed to higher cell viability (>80%) at concentrations of 1, 10, and 100 µg/mL compared to the UV-exposed control. Furthermore, the kale extracts and all tested phytochemicals (0.001-100 µg/mL) significantly reduced UV-induced reactive oxygen species ($p < 0.05$) compared to the UV-treated control. UV irradiation increased DNA damage, while K(U) at 0.01 and 0.1 µg/mL, chlorogenic acid at 0.1 µg/mL, and sulforaphane at 0.001 and 0.01 µg/mL significantly reduced DNA damage compared to the UV-treated control, as determined using phosphorylated H2A histone (γ-H2AX) immunofluorescence assay. Therefore, phytochemical-rich kale extracts demonstrate potential in protecting skin fibroblasts from UV-induced oxidative stress and DNA damage, suggesting potential applications in cosmeceutical formulations for skin protection against UV radiation.

Keywords: Food bioactives; *Brassica oleracea* var. acephala; Skin health; Phytochemicals; Cosmeceuticals.

1. Introduction

Ultraviolet (UV) radiation is a major contributor to skin cancer, which remains a public health concern in Canada (De Almeida et al., 2022; Tang et al., 2024). In 2022, skin cancer accounted for approximately one-third of all newly diagnosed cancer cases in Canada (Moskwa et al., 2023). Exposure to UV radiation (UVR), particularly UVB, damages the epidermal basal layer, leading to mutations and skin cancer (Hegedűs et al., 2021). Whereas UVA penetrates deeper due to its longer wavelength, generating reactive oxygen species (ROS) that disrupt homeostasis and accelerate skin aging (Bernerd et al., 2022). Excessive ROS results in oxidative damage and activates pro-tumorigenic signaling, leading to genome instability (Kozlov et al., 2024).

Bioactive phytochemicals, such as (poly)phenols, carotenoids, and glucosinolates, contribute to the removal or scavenging of ROS (Oyerinde et al., 2025). Low levels of ROS can also activate antioxidant enzymes and contribute to oxidative homeostasis (Kobayashi et al., 2025). The American Cancer Society recommends a diet rich in dark green, orange, and red vegetables, which provide

essential nutrients and bioactive phytochemicals for cancer prevention (Rock et al., 2020). Among these, kale (*Brassica oleracea* var. *acephala*) is a nutrient- and bioactives-dense leafy vegetable known for its high carotenoid content, which can combat oxidative stress and UV-induced skin DNA damage (Ortega-Hernández et al., 2021). (Poly)phenols in kale extracts possess strong antioxidant properties that help in preventing oxidative stress and DNA damage (Valisakkagari et al., 2024). Among the major bioactive phytochemicals in cruciferous vegetables such as cabbage and kale, sulforaphane is reported to activate the nuclear factor erythroid 2–related factor 2 (Nrf2) signaling pathway, thereby upregulating antioxidant enzymes and enhancing cellular defense against ROS and DNA lesions (Alves et al., 2025). Chlorogenic acid, another important constituent, offers potent antioxidant and DNA-protective benefits by efficiently scavenging free radicals and supporting endogenous defense systems such as the glutathione pathway (Lee et al., 2021). Together, these components enable kale extracts to decrease ROS accumulation, alleviate oxidative stress, and provide enhanced cryoprotection against UV-induced cellular damage. Recently, interest in upcycling and valorizing expired, surplus, and rejected kale for value-added product development has been emerging (Valisakkagari et al., 2024).

Several *in vitro* and *in vivo* experiments, including animal studies and human trials, have demonstrated the protective effects of (poly)phenols and carotenoids against UV-induced oxidative stress and skin aging (Balić and Mokos, 2019). Human trials with oral supplementation of carotenoid-rich extracts have shown improved skin hydration, elasticity, and resistance to UV-induced damage (Groten et al., 2019). Additionally, bioactive phytochemicals from kale, including flavonoids and isothiocyanates, have been demonstrated to possess potential effects in preventing skin aging by modulating inflammatory pathways and enhancing collagen synthesis (Wang et al., 2020). These findings conclude that carotenoids, (poly)phenols, and sulforaphane have the potential to be incorporated into cosmeceutical products.

Reports on the antioxidant properties of phytochemical-rich extracts prepared using upcycled kale remain scarce. Therefore, this study investigated the protective effects of bioactive phytochemicals extracted from upcycled kale against UV-induced oxidative stress and DNA damage in human skin fibroblasts (WS1 cells) in vitro.

2. Materials and methods

2.1. Chemicals and reagents

Primary antibody anti-phospho-histone γ-H2AX mouse (ser139) (cat. no. 05-636) was obtained from Sigma-Millipore (Etobicoke, ON, Canada). Secondary antibody Alexa Fluor® 594 donkey anti-mouse (cat. no. A-21203) was obtained from Thermo Fisher Scientific (Chelmsford, MA, USA). was purchased from Sigma® Life Science (St. Louis, MO, USA). Fetal bovine serum (FBS) (cat. no. 12483-020), Tris base/boric acid/ethylenediaminetetraacetic acid (EDTA) (TBE) buffer (cat. no. B52), Tween 20 (cat. no. 9005-64-5) were obtained from Thermo Fisher Scientific (Chelmsford, MA, USA). Minimum Essential Eagle's Medium (cat. no. M2279), 2′7′-dichlorofluorescein diacetate (DCFDA) (cat. no. D6883), 0.25% Trypsin–EDTA (cat. no. T3924), bovine serum albumin (BSA) (cat. no. A8022), dimethylsulfoxide (DMSO) (cat. no. 276855), polyvinylepyriilodone (cat. no. P0930), paraformaldehyde (cat. no. P6148), penicillin-streptomycin cat. no. P0781), phenazine methosulfate (PMS) (cat. no. P9625), Triton X-100 (cat. no. T8787), chlorogenic acid (cat. no. C3878), quercetin (cat. no. Q4951-109), and sulforaphane (cat. no. 4478-93-7) were obtained from Sigma-Aldrich (Oakville, ON, Canada). Lutein (cat. no. B0005-465469) from BOC Sciences (New York, NY, US). MTS (3-(4,5-dimethylthiazol-2-yl)-5-(3-carboxymethoxyphenyl)-2-(4-sulfophenyl)-2Htrazolium) reagent (cat. no. G1111) was obtained from Promega (Madison, WI, USA). Vectashield® containing 4′,6-diamidino-2-phenylindol (DAPI) (cat. no. H-1200) was obtained from Vector Laboratories Inc. (Burlingame, CA, USA). Dulbecco's phosphate-buffered saline (PBS) (cat. no. 02-0119-1000) was obtained from VWR Life Sciences (Edmonton, AB, Canada). All the chemicals used in this study were suitable for cell-based experiments.

2.2. Preparation of the extracts

The bioactive phytochemical-rich extracts of K(M) and K(U) were prepared using microwave-assisted extraction and ultra-sonication-assisted extraction, respectively, using a previously described method (Valisakkagari and Rupasinghe 2025). These two extraction methods yielded the highest total carotenoids, total phenolics and total antioxidant capacity when compared to those of other tested extraction methods (Valisakkagari and Rupasinghe 2025). Briefly, the upcycled kale powder was prepared using the vacuum-drying method at Outcast Foods Ltd (Dartmouth, NS, Canada) using expired and surplus kale collected from local grocery stores. For the experiment, 300 g samples were collected from three lots were mixed thoroughly before use for the extraction. The ultrasound-assisted extraction conditions were 1 g to 20 mL of 100% ethanol at 57 °C for 30 min (Model 4HT-1524-12, Crest, Ewing, NJ, USA). Microwave-assisted extraction was performed using 1 g in 10 mL of 80% ethanol at 450 W for 2 min (The Genius microwave 1100W Model NNSG676W, Panasonic, Boston, MA). The solvents of both extracts were completely removed using nitrogen flushing, and the dried pellets were dissolved in dimethyl sulfoxide (DMSO) for use in cell-based assays.

2.3. Instruments

UV crosslinker AH, 115 V (Model 234100), UVA lamp (368 nm, color black), and UVB lamp (306 nm, color white) were purchased from Boekel Scientific Inc. (Pennsylvania, PA, USA). Fourier transform infrared spectrophotometer (Spectrum Two FT-IR, Model L1600300LITA; PerkinElmer Inc., Llantrisant, UK) and ultra-performance liquid chromatography-electrospray ionization-mass spectrometry system (UPLC-ESI-MS, Acquity UPLC H-class; Waters Limited Inc., Milford, MA, USA) equipped with an electrospray ionization tandem quadrupole mass spectrometer detector (ESI-MS-MS, Quattro Micro; Waters Limited Inc., Milford, MA, USA) were used to detect pure phytochemicals. Biological safety cabinet (Class II, Model LR2-452; ESCO Technologies Inc., Missouri, USA), water bath (Model ISOTEMP 205; Fisher Scientific, Waltham, MA, USA), CO_2 incubator (Model 3074; VWR International, Radnor, PA, USA), centrifuge (Sorvall Legend Micro 21 R; Thermo Fisher Scientific Inc., Waltham, MA, USA), inverted microscope (Eclipse TS100F; Nikon Instruments Inc., Cambridge, MA, USA), microplate reader (Model M200 PRO; Tecan Infinite®, Morrisville, NC, USA), mini shaker (Model 980334; VWR International, Radnor, PA, USA), freeze dryer (Dura-Dry, Model 14-85BMP1; DJS Enterprises Inc., Cincinnati, OH, USA), microcentrifuge (Sorvall ST 16; Thermo Fisher Scientific Inc., Waltham, MA, USA), and glass coverslips (1.5, 22 × 22 mm,

Cat. No. B10143263NR15; VWR International, Radnor, PA, USA) were used in the study.

2.4. Methods

2.4.1. FT-IR spectral analysis

The kale extracts and pure phytochemicals (lutein, chlorogenic acid, quercetin, and sulforaphane) were analyzed to identify their chemical bonds and molecular structure using FT-IR (Spectrum Two FT-IR Spectrophotometer Model L1600300LITA, PerkinElmer, Llantrisant, UK). An aliquot of approximately 1 mg of the sample was placed directly onto the ATR (Attenuated Total Reflectance) crystal for measurement. Spectral data were acquired by scanning from 4,000 - 400 cm^{-1} at a spectral resolution of 4 cm^{-1}. The obtained spectra were analyzed to identify characteristic peaks corresponding to functional groups by comparing them with reference spectra (Quijano-Ortega et al., 2020).

2.4.2. UPLC-ESI-MS analysis

The UPLC-ESI-MS analysis was conducted to quantify major bioactive phytochemicals of K(M) and K(U) using a previously described method (Valisakkagari and Rupasinghe 2025). Briefly, sample extracts were filtered through 0.2 µm nylon filters, placed in amber vials, and injected (5 µL volume) into a reverse-phase Waters BEH C18 column (2.1 × 100 mm, 1.7 µm) at a flow rate of 0.2 mL/min. Chromatographic separation was achieved using a linear gradient of 0.1% formic acid in water (solvent A) and 0.1% formic acid in acetonitrile (solvent B). The Micromass Quattro Micro-API MS/MS system operated with an ESI source temperature of 375 °C and a capillary voltage of 3,000 V. Quantification relied on calibration curves created from analytical standards (purity >98%). The major analytes and their respective m/z values were lutein (ESI+; m/z 568.8), β-carotein (ESI+; m/z 536.5), sinigrin (ESI+; m/z 568.8), glucobrassicin (ESI-; m/z 446.9), DL-sulforaphane (ESI+; m/z 179), kaempferol (ESI−; m/z 285.2), quercetin (ESI−; m/z 300.7), chlorogenic acid (ESI−; m/z 353.2), and ferulic acid (ESI-; m/z 193.08).

2.4.3. Skin fibroblast cultures

The human skin fibroblast cell line, WS1 (ATCC CRL-1502 ™) was purchased from American Type Culture Collection (ATCC) (Manassas, VA, USA). WS1 cells were grown in EMEM supplemented with 10% FBS, 4 mM L-glutamine, 100 µg/mL streptomycin and 100 U/mL penicillin. The cell culture was maintained at 37 °C in a humidified incubator with 5% CO_2 and sub-cultured before reaching confluency. A T-75 cell culture flask containing a monolayer of WS1 cells was washed with PBS following the aspiration of the media. A 0.25% Trypsin-EDTA solution containing 0.5% polyvinylpyrrolidone was added to the culture flask, and cells were incubated for 2 min at 37 °C with 5% CO_2 until detachment. The detached cells were aspirated and transferred into a centrifuge tube, and complete EMEM medium was added to neutralize trypsin activity. The cell suspension was centrifuged (350 × g) for 5 min, and the pellet was resuspended in fresh complete EMEM medium and transferred to a new T-75 flask. Experiments were conducted using cells at 80–85% confluency, between passages 2 and 15.

2.4.4. Cell viability using MTS assay

For MTS assay, WS1 cells were seeded at 1×10^4 cells per well in 96-well tissue culture plates and incubated for 24 h until reaching approximately 80% confluency. Cells were then incubated with test compounds, including two kale extracts of K(U) and K(M), lutein (LU), chlorogenic acid (CA), quercetin (QN), and sulforaphane (SFN). To induce oxidative stress, cells were exposed to UVA (252 nm, black bulbs) and UVB (306 nm, white bulbs) radiation using a UV crosslinker. The optimal UV exposure parameters were predetermined, and WS1 cells were irradiated at 0.89 J/cm^2 for 2 min. Following the 24 h incubation with test compounds, MTS reagent was added to each well, and the plates were incubated for 3 h in the dark. The absorbance was measured at 490 nm using an plate reader (Infinite® 200 PRO, TECAN, Mannedorf, Switzerland) (Amararathna et al., 2020).

2.4.5. Measurement of intracellular ROS

To measure intracellular ROS levels, WS1 cells were employed with a cell-permeable probe called 2′,7′-dichlorofluorescin diacetate (DCFDA). Cells were seeded (1×10^4 cells per well) in black-sided clear-bottom 96-well microplates and incubated at 37 °C in a humidified incubator with 5% CO_2. Then, cells were incubated with different concentrations (0.1, 1, 10, 100 µg/mL) of K(U), K(M), LU, CA, QN, and SFN for 24 h. After incubation, cells were exposed to UVR using a UV crosslinker (Boekel Scientific, Feasterville, PA), equipped with UVA and UVB for 2 min at 0.89 J/cm^2. A 5 µM DCFH-DA working solution was added to the treated cells and incubated in the dark for 30 min. The intracellular ROS levels were quantified by measuring fluorescence at an excitation wavelength of 485 nm and an emission wavelength of 535 nm using a plate reader (Infinite® 200 PRO, TECAN, Mannedorf, Switzerland). DCFDA is a non-fluorescent molecule that diffuses through cell membranes and is hydrolyzed intracellularly. Upon oxidation by ROS, DCFDA forms 2′,7′-dichlorofluorescein (DCF). The fluorescent intensity of DCF is directly proportional to the ROS levels (Suraweera et al., 2020).

2.4.6. γ-H2AX immunofluorescence assay

For quantifying γ-H2AX foci, WS1 cells were seeded at 1×10^5 cells per well on sterilized, coated coverslips placed in a 6-well plate and incubated for 24 h. Following treatment with K(U), K(M), LU, CA, QN, and SFN of (0.001, 0.01, 0.1 mg/mL) for 24 h. After the treatments, the cells were rinsed with 1 × PBS and then treated with 3.7% paraformaldehyde for 20 min in the dark. Cells were then permeabilized with 0.5% Triton X-100 in PBS for 15 min at room temperature and blocked with 4% BSA for 20 min to prevent non-specific binding. Coverslips were incubated with a primary anti-phospho-histone H2AX antibody (1:250) for 1 h, rinsed three times with PBS, and then incubated with a secondary Alexa Fluor® 594 donkey anti-mouse antibody (1:500) for 45 min in the dark. The coverslips were washed three times with 1 × PBS to remove excess secondary antibodies. After washing with PBS, coverslips were mounted onto glass slides using Vectashield® containing 4′,6-diamidino-2-phenylindol (DAPI) and sealed with transparent nail polish. Slides were imaged at 150 × magnification using a fluorescence microscope (EVOSTM FLoid Imaging System, Bothell, WA, USA), and Fiji ImageJ software (Version 1.54p, NIH, Bethesda, MD, USA) was used to quantify γ-H2AX foci for at least 50 nuclei per treatment (Amararathna et al., 2020).

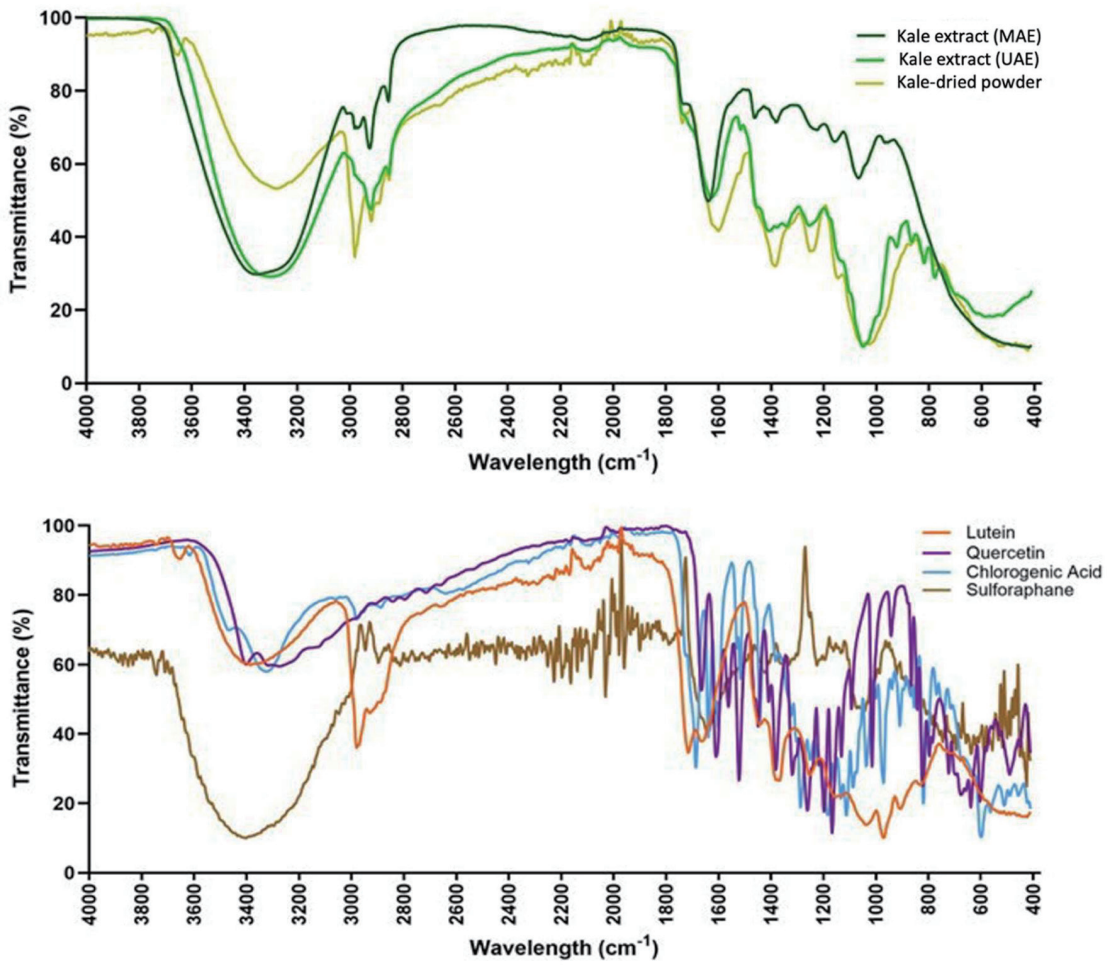

Figure 1. FT-IR analysis representing the upcycled kale powder, extracts of UAE and MAE, and major phytochemical constituents (lutein, chlorogenic acid, quercetin, and sulforaphane).

2.5. Statistical Analysis

The experiments mentioned were conducted in triplicate and repeated three times ($n = 9$). Statistical analysis was performed using Minitab (Version 22, Minitab, LLC, State College, PA, USA). Data were first tested for primary assumptions for analysis of variance (ANOVA). One-way ANOVA was conducted to determine statistical significance, followed by Tukey's post-hoc test for multiple mean comparisons. A 95% confidence interval ($p < 0.05$) was considered statistically significant. The graphs for the experiments were generated by GraphPad Prism software (San Diego, CA, USA), and error bars represent standard deviation across all analyses to ensure the reliability of the results.

3. Results and discussion

3.1. FT-IR spectral analysis for upcycled kale extracts

The FT-IR spectra of upcycled kale extracts obtained by UAE and MAE, in comparison to the major bioactive phytochemicals of kale (LU, CA, QN, and SFN) were analyzed for functional groups (Figure 1). Both extraction methods showed a broad O-H stretching peak (UAE: 3,350 cm^{-1}, MAE: 3,305 cm^{-1}), indicating alcohols and carboxylic acids, likely phenolic compounds. However, the observed O-H streaking could also be due to the water of the aqueous extract. The C-H stretching peaks (UAE: 2,918 cm^{-1}, MAE: 2,924 cm^{-1}) suggest alkanes or saturated hydrocarbons, while the strong C=O stretching (UAE: 1,625 cm^{-1}, MAE: 1,636 cm^{-1}) region to esters or carboxylic acids. The differences in C-O stretching (1,200–1,000 cm^{-1}) suggest variations in extraction efficiency (Manzoor et al., 2019). These findings agree with previous studies confirming the presence of (poly)phenols and flavonoids (Murugesan et al., 2021). Compared to vacuum-dried kale powder, extracts exhibited distinct peaks in the fingerprint region, indicating a more diverse composition. The kale powder and extracts may contain the same phytochemicals; however, the extraction process enhanced the visibility of functional groups, producing more concentrated bioactive phytochemicals for analysis (Abedelmaksoud et al., 2025).

The FT-IR spectrum of lutein showed a strong C=C stretching peak at 1,664 cm^{-1}, characteristic of carotenoids, with C-O stretching at 1,366 cm^{-1} and 1,036 cm^{-1}, likely from oxygenated compounds. Kale extracts containing QN and CA showed a broad O-H stretching band (~3,300 cm^{-1}), characteristic of phenolics, with

Table 1. Quantitative analysis of major bioactive phytochemicals in upcycled kale extracts obtained by UAE and MAE using ethanol as solvent

Bioactive Phytochemicals (µg/g DW)	Ultrasound-Assisted Extraction (UAE)	Microwave-Assisted Extraction (MAE)
Lutein	879 ± 125[b]	1,229 ± 369[b]
β-carotene	947 ± 95.7[a]	492 ± 63[b]
Sinigrin	73.1 ± 10.5[c]	457 ± 12.2[a]
Glucobrassicin	3.54 ± 0.79[b]	85.0 ± 3.48[a]
DL-Sulforaphane	2,656 ± 82.7[b]	2,891 ± 73.4[b]
Kaempferol	2.83 ± 1.06[a]	2.79 ± 0.59[a]
Quercetin	73.2 ± 13.8[b]	267 ± 21.3[a]
Chlorogenic acid	84.4 ± 20[b]	536 ± 18.1[a]
Ferulic acid	92.2 ± 2.9[c]	146 ± 11.8[b]
Total Phytochemicals	4,811	6,106

Data represent mean ± standard deviation. DW, dry weight; MAE, microwave-assisted extraction; UAE, ultrasound-assisted extraction.

stronger C=O absorption in CA (1,700–1,600 cm^{-1}, 1,047 cm^{-1}), indicating conjugated carbonyl groups. The FT-IR spectrum of SFN differed from that of kale extracts in its analysis of organosulfur functional groups due to spectral noise.

To complement the FT-IR spectral findings above, UPLC-ESI-MS analysis was performed to quantify major bioactive phytochemicals, including LU, CA, QN, and SFN, in upcycled kale extracts obtained by UAE and MAE (Valisakkagari and Rupasinghe 2025) (Table 1). The K(M) exhibited significantly higher concentrations of these bioactive phytochemicals than those of K(U). The quantitative results of UPLC-ESI-MS support the FT-IR evidence of enriched bioactive phytochemicals, particularly (poly)phenols, and carotenoids in the extracts.

By integrating these two analytical approaches, FT-IR provides a rapid overview of the functional groups present, while UPLC-ESI-MS analysis delivers precise profiling and quantification of specific bioactive phytochemicals. Together, these methods demonstrate the effectiveness of the extraction techniques, with MAE showing higher recovery of diverse bioactive phytochemicals from upcycled kale.

3.2. Evaluation of UV-induced cytotoxicity in WS1 cells measured by MTS assay

Cell viability of the extracts and test compounds (1, 10, and 100 µg/mL) was assessed using the MTS colorimetric assay under experimental conditions. The upcycled kale extracts K(U) and K(M) maintained cell viability (>80%) across all tested concentrations without significant dose-dependence effect ($p > 0.05$) (Figure 2).

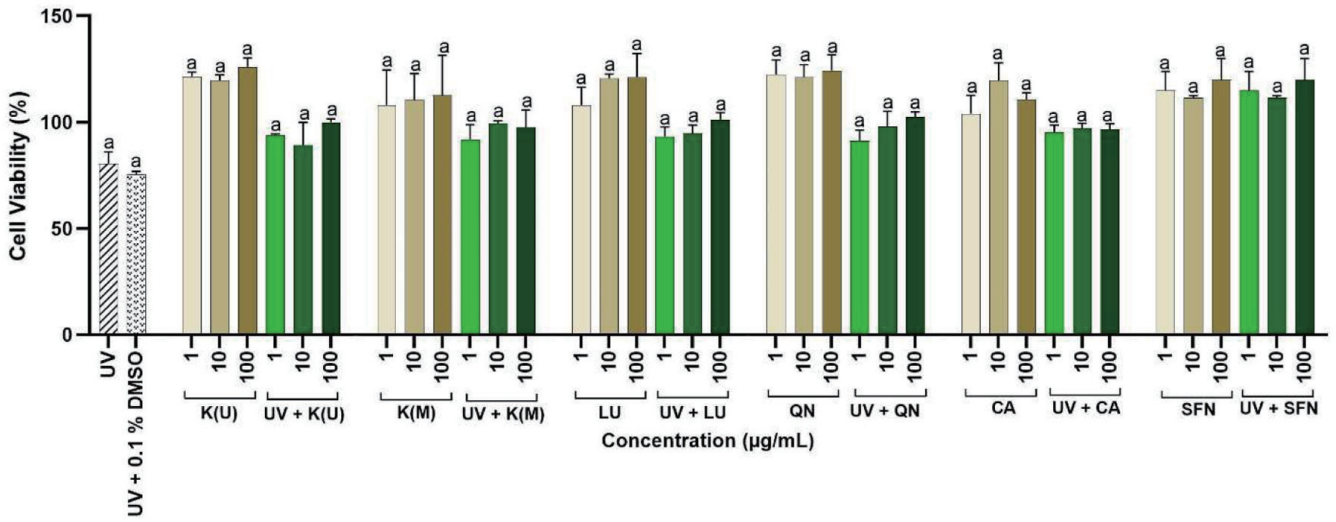

Figure 2. Viability of WS1 cells pre-treated with extracts of ultrasound-assisted extraction [K(U)] and microwave-assisted extraction [K(M)], and selected phytochemicals. The extracts, lutein (LU), chlorogenic acid (CA), quercetin (QN), and sulforaphane (SFN) were incubated at 1, 10, and 100 µg/mL concentrations for 24 h. Cells were then exposed to UVR for 2 min at 0.89 J/cm^2, and cell viability was assessed using the MTS assay. Cell viability is expressed as a percentage relative to the UVR control. Experimental results are shown as mean ± SD of three independent experiments (n = 9). The analysis was performed using one-way ANOVA, followed by Tukey's pairwise comparison test ($p < 0.05$) using Minitab (Version 22, Minitab, LLC, State College, PA, USA) and GraphPad Prism software (San Diego, CA, USA). The letters (a and b) represent the statistical differences between the tested compounds ($p < 0.05$). The same letter for the means is not significantly different at ($p < 0.05$).

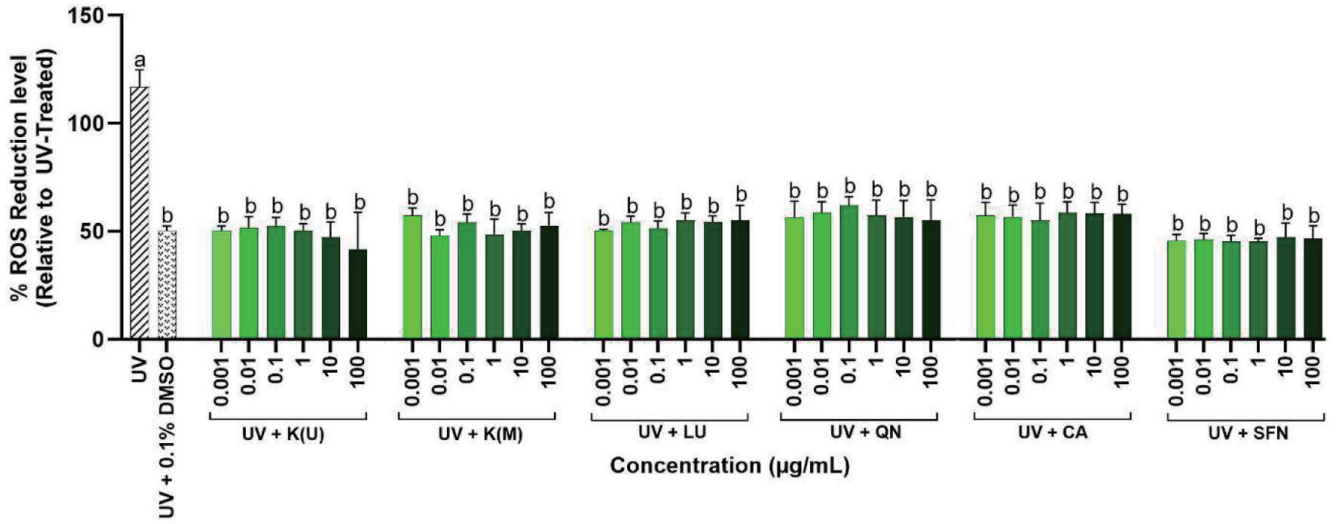

Figure 3. The reduction of reactive oxygen species (ROS) of UV-radiation induced WS1 cells by kale extracts [K(M) and K(M)], lutein (LU), quercetin (QN), chlorogenic acid (CA), and sulforaphane (SFN), The test compounds were incubated at concentrations of 0.001, 0.01, 0.1, and 1 µg/mL for 24 h, followed by UV irradiation (0.89 J/cm^2 for 2 min). ROS levels were quantified using the DCFDA assay and are expressed as a percentage of ROS relative to the UV control. Data are presented as the mean ± standard deviation from three independent experiments (n=9). The significant difference was determined by one-way ANOVA followed by Tukey's test ($p < 0.05$) using Minitab (Version 22, Minitab, LLC, State College, PA, USA) and GraphPad Prism software (San Diego, CA, USA). Treatments with error bars (different letters) are statistically significantly different.

Similarly, lutein, quercetin, chlorogenic acid, and sulforaphane exhibited consistently high cell viability (>90%), with no significant differences among tested concentrations ($p > 0.05$) as shown in Figure 2.

The MTS assay defined the cell viability by reducing the tetrazolium compound into a soluble purple formazan product, providing measures for the cytotoxicity of test compounds (Stefanowicz-Hajduk and Ochocka, 2020). Given that UV irradiation induces oxidative stress, the ability of the bioactive phytochemicals to maintain high cell viability suggests their potential as photoprotective agents (Tomas et al., 2025). The findings suggest that the lack of cytotoxicity for K(U) and K(M) extracts may reflect effective mitigation of UV-induced cellular DNA damage, probably through antioxidant mechanisms (Budzianowska et al., 2025). Studies related to UV-induced human skin fibroblasts *in vitro* for LU, CA, QN, and SFN demonstrated a concentration-dependent effect on cell viability (Rajnochová Svobodová et al., 2022; Xue et al., 2022). Herein, prior studies have shown that the test compounds used in this study can reduce ROS levels and prevent DNA damage in UV-exposed skin fibroblasts (Anbualakan et al., 2022; Calniquer et al., 2021). Therefore, all tested concentrations showed no significant dose-dependent effect, suggesting that they may be effectively used further for UV-induced cellular DNA damage experiments.

3.3. Evaluation of upcycled kale extracts and selected phytochemicals against UV-induced ROS levels

Oxidative stress induced by UVR causes DNA damage and cellular dysfunction, primarily through the generation of ROS (Sies and Jones, 2020). Bioactive phytochemicals are known to mitigate these effects by scavenging ROS and enhancing cellular defense mechanisms (Lagunas-Rangel and Bermúdez-Cruz, 2020). This study investigated the protective effects of kale extracts (K(U) and K(M)) along with their major phytochemical constituents against UV-induced DNA damage *in vitro*, as measured by ROS generation in WS1 cells. Our results indicate that all tested compounds (0.001–100 µg/mL) significantly reduce ROS levels compared to the UV-treated group ($p < 0.05$) (Figure 3). However, there is no significant difference in ROS reduction across the tested concentrations or between the different compounds ($p > 0.05$). Consistent with prior research, *Houttuynia cordata* extracts reduced UVB-induced ROS by 35–61% in skin fibroblast cells, attributed to flavonoids like quercitrin and hyperoside, which scavenged radicals and upregulated antioxidant enzymes (Mapoung et al., 2021). Interestingly, the 0.1% dimethyl sulfoxide (DMSO) significantly lowered ROS levels relative to UV-treated cells ($p < 0.05$), indicating the inherent antioxidant properties of DMSO (Bulama et al., 2022). However, DMSO dose-dependent effect concentration ≤ 0.5% led to a reduction in ROS activity, and high dose (3.7%) increased ROS and apoptosis in H9c2 cardiomyoblasts (Sangweni et al., 2021). DMSO scavenges hydroxyl radicals (HO·), moderately reducing UV-induced oxidative DNA damage such as 8-oxo-7,8-dihydro-2′-deoxyguanosine (8-oxo-dG) by neutralizing HO· involved in guanine oxidation (Chatgilialoglu et al., 2021). While DMSO scavenges HO·, its derivatives, such as methyl radicals, appear to contribute to DNA double-strand breaks oxidative stress (Noda et al., 2017). The DMSO remains a "gold standard" solvent for cell-based assays.

The minimal variance between concentrations within each compound group may indicate saturation kinetics, where cellular antioxidant capacity is reached at lower concentrations (Jomova et al., 2024). It is also possible that some cell types have low esterase activity, limiting their ability to detect ROS at lower concentrations, as DCFH-DA needs to be hydrolyzed (Eruslanov and Kusmartsev, 2010). Despite these limitations, tested bioactive phytochemicals (LU, QN, CA, and SFN) significantly reduced ROS levels in UV-irradiated WS1 fibroblasts, consistent with previous findings in other experimental models (Calniquer et al., 2021). This shows that the effects of bioactive phytochemicals can vary depending on cell type and stress-specific effects (Zheng et al., 2020). The ROS

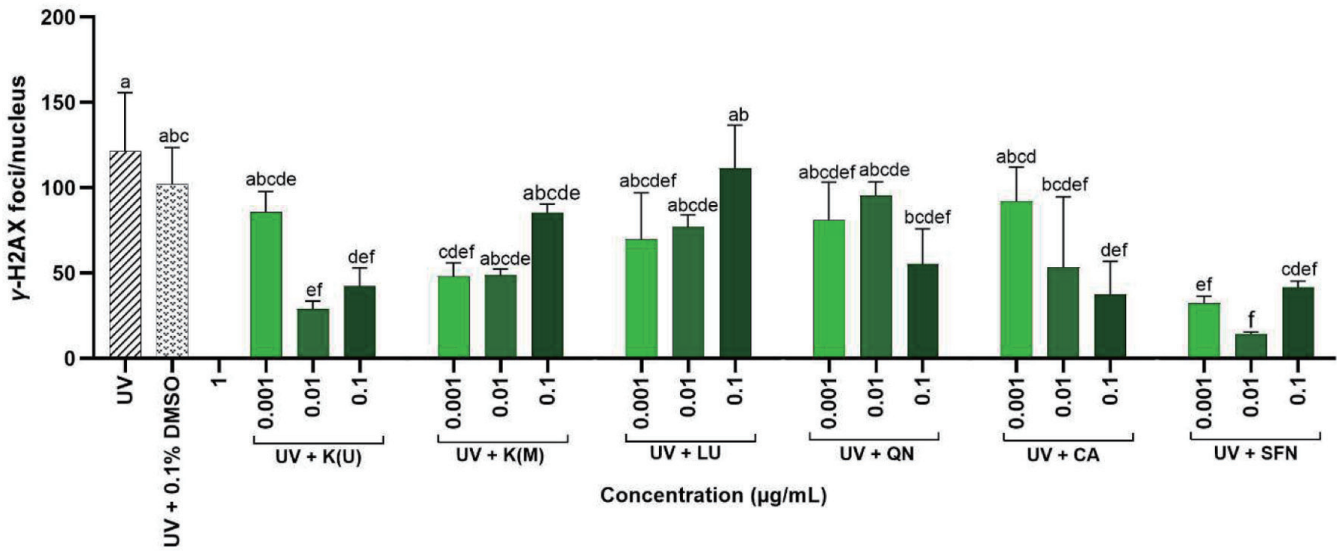

Figure 4. Protection of DNA damage of UV radiation-induced WS1 cells by kale extracts and phytochemicals as measured by γ-H2AX immunofluorescence assay. The ES1 cells were pre-treated for 24 h with the extracts of ultrasound-assisted extraction [K(U)] and microwave-assisted extraction K(M)], lutein (LU), chlorogenic acid (CA), quercetin (QN), and sulforaphane (SFN) at three concentrations (0.001, 0.01, and 1 µg/mL) with vehicle control (0.1% DMSO). Cells were then exposed to UVR (0.89/cm^2) for 2 min. DNA damage was assessed by immunofluorescence staining for γ-H2AX, a marker of DNA double-strand breaks. The number of γ-H2AX foci per nucleus was quantified using Fiji ImageJ software (Version 1.54p, NIH, Bethesda, MD, USA), with at least 50 cells counted per treatment. The experiments were performed in three independent times in triplicate (n = 9), and results are expressed as mean ± standard deviation. Statistical analysis was performed by one-way ANOVA, and mean comparison was done by Tukey's multiple comparisons test (α = 0.05) using Minitab (Version 22, Minitab, LLC, State College, PA, USA) and GraphPad Prism software (San Diego, CA, USA). Mean values that do not share similar letters in bar graphs are considered as significantly different ($p < 0.05$).

reduction levels for all compounds are similar, with no marked superiority of one compound over another in reducing ROS caused by UV exposure.

3.4. Evaluation of DNA double-strand breaks using γ-H2AX histone marker

UV-induced DNA damage leads to double-strand breaks, as indicated by γ-H2AX foci formation. In this study, the UV-exposed cells (the experimental model of DNA damage) showed a high level of γ-H2AX foci, indicating significant DNA damage (Figures 4 and 5). The 0.1% DMSO control did not significantly alter γ-H2AX levels relative to the UV-treated group, suggesting that the solvent itself had neither a protective nor a damaging effect at this concentration. The K(U) at 0.01 and 0.1 µg/mL, CA at 0.1 µg/mL, and SFN at 0.001 and 0.01 µg/mL significantly reduced γ-H2AX foci compared to the UV control. Thus, K(U) effectively mitigate UV-induced DNA damage and its protective effect on skin fibroblasts. The reduction in H2AX foci after exposure to UV and pre-treatment with K(U) may be attributed to enhanced DNA repair mechanisms and direct scavenging of ROS. CA at 3 µM decreased UVA-induced γ-H2AX foci and upregulated collagen synthesis while inhibiting MMPs, against DNA damage and photoaging in human dermal fibroblasts (Xue et al., 2022). SFN at lower doses (0.001–0.01 µg/mL) protected against DNA damage, where low dose stimulation (<10 µM) activates the Nrf2 pathway, enhancing antioxidant defenses and protecting against UV-induced oxidative damage (Calabrese and Kozumbo, 2021). This was similarly observed with a previous study, which reported that SFN pre-treatment reduced γ-H2AX foci following ionizing radiation (Mathew et al., 2014).

In contrast, LU and QN did not show a significant reduction in γ-H2AX foci at any concentration tested. It indicates that, under the conditions of our experiment, these compounds do not provide protection against UV-induced DNA damage measured by γ-H2AX formation. This can be possible to differences in cellular uptake or mechanisms of action compared to the other tested compounds. Lutein cellular absorption is reduced when co-administered with flavonoids, for example, luteolin or quercetin, as seen in summarized *in vitro* models, potentially diminishing its protective effects against UV-induced DNA damage (Chen et al., 2021). A study have demonstrated the potential of carnosol (phenolic compound) to reduce γ-H2AX foci and checkpoint kinase 1 (Chk1) phosphorylation in UVB-induced cells, indicating that a synergistic effect contributes to their protective effect, which is absent when compounds are tested individually, similar to our experiment (Tong and Wu, 2018). To conclude, this study demonstrates that upcycled kale extracts reduced γ-H2AX formation, showing their protective effect against UV-induced DNA damage. Furthermore, future research can be focused on additional biomarkers of DNA damage and their mechanism of action to explore long-term skin health applications.

4. Future directions

The study extended to evaluate the phytochemical-rich kale extracts for their ability to reduce oxidative stress and protect skin fibroblasts (WS1 cells) against UV-induced DNA damage *in vitro*. The results indicated that the kale extracts and selected phytochemicals at physiological concentrations maintained cell viability. All the test compounds exhibited notable antioxidant activity by significantly reducing ROS levels. Furthermore, K(U) at 0.01

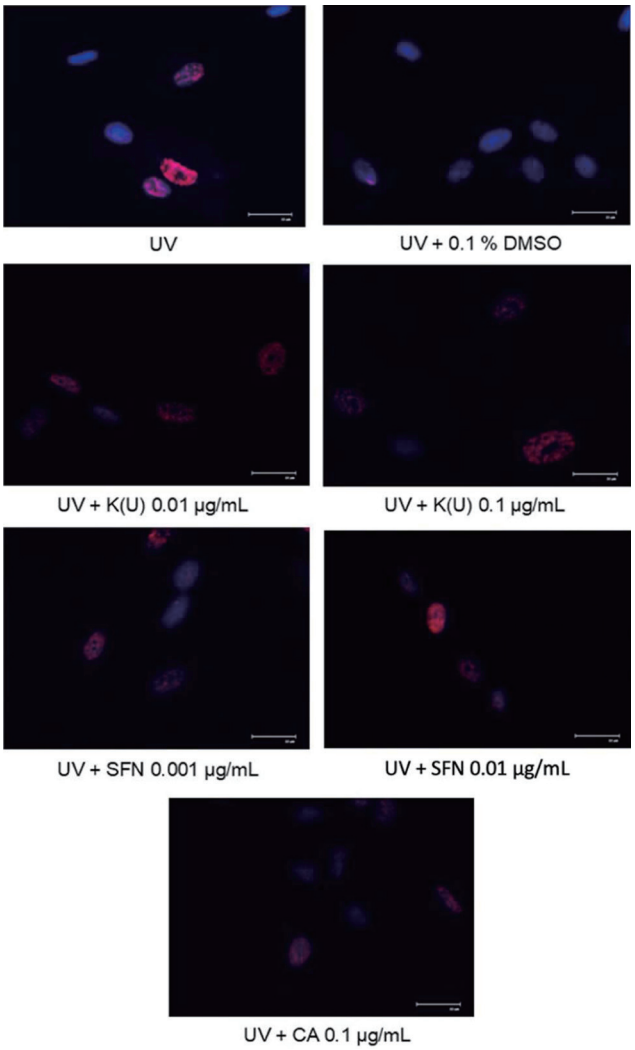

Figure 5. Upcycled kale extract [K(U)], CA, and SFN reduced the UV-induced DNA damage analyzed by the γ-H2AX immunofluorescence assay. Cells were treated with UV (the model) and DMSO (solvent control), and the indicated concentrations of compounds K(U), CA, SFN in combination with UV. The γ-H2AX foci are shown in red, and nuclei are stained with DAPI (blue). Slides were imaged at 150× magnification using a fluorescence microscope.

and 0.1 µg/mL effectively reduced UV-induced DNA damage, as evidenced by γ-H2AX immunofluorescence analysis. These findings suggest that phytochemical-rich extracts from upcycled kale obtained through the UAE method possess the capacity to protect skin cells from UV-induced oxidative stress and DNA damage. Thus, bioactive phytochemical-rich extracts of upcycled kale may be useful for developing cosmeceutical products aimed at protecting skin from UVR (Jesus et al., 2023). The study addresses the global concern of food waste reduction while simultaneously promoting the principles of the circular economy and reducing reliance on synthetic compounds. By repurposing food industry by-products, the study demonstrates an innovative approach to sustainable resource management in the cosmeceutical sector.

To further validate the findings from *in vitro* studies, it is recommended to conduct additional in-depth analyses, such as 8-oxoG quantification, comet assay, and western blot analysis, to elucidate the molecular mechanisms, such as the regulation of Nrf2 pathway, underlying the protective effect of phytochemical-rich kale extracts against UV-induced DNA damage (Kciuk et al., 2020; Suraweera et al., 2020). While *in vitro* models provide fundamental insights, *in vivo* studies using hairless mouse models such as SKH-1 (senescence-accelerated hairless mouse 1) or HR-1 (hairless mouse 1), are recommended. These models are widely used to evaluate biomarkers of DNA damage and oxidative stress in a more complex biological system (Anbualakan et al., 2022). Further, performing comprehensive safety and efficacy testing to meet the regulatory requirements for cosmetic products should be considered. Therefore, these studies will bridge the gap between clinical studies and human applications, providing compelling evidence for integrating upcycled kale extracts to improve skin health.

5. Conclusion

This study suggests that bioactive phytochemical-rich extracts of upcycled kale have the potential to protect WS1 skin cells from UV-induced DNA damage. The kale extract produced from UAE significantly reduced γ-H2AX foci, a biomarker of DNA double-strand breaks. While all tested phytochemicals effectively reduced UV-induced ROS levels, the 0.1% DMSO control exhibited a similar ROS reduction compared to the tested compounds. The study found that bioactive phytochemicals such as β-carotene and sulforaphane had a significant impact on UV-induced DNA damage, suggesting their role in the extract. Furthermore, integrating FT-IR and UPLC-ESI-MS analysis confirmed the higher recovery of a broad spectrum of bioactive phytochemicals from upcycled kale, demonstrating their potential applications in functional foods, nutraceuticals and cosmeceuticals. The findings suggest potential for the development of cosmeceutical ingredients using upcycled kale to reduce the risk of skin cancer. Further studies could address the limitations of *in vitro* studies and validate these preliminary findings using *in vivo* and/or human clinical trials.

Acknowledgments

The authors would like to acknowledge the Natural Resources and Engineering Research Council (NSERC) of Canada (ALLRP 570618-21) for the financial support.

References

Abedelmaksoud, T.G., Younis, M.I., Altemimi, A.B., Tlay, R.H., and Ali Hassan, N. (2025). Bioactive Compounds of Plant-Based Food: Extraction, Isolation, Identification, Characteristics, and Emerging Applications. Food Sci. Nutr. 13: e70351.

Alves, I., Araújo, E.M.Q., Dalgaard, L.T., Singh, S., Børsheim, E., and Carvalho, E. (2025). Protective Effects of Sulforaphane Preventing Inflammation and Oxidative Stress to Enhance Metabolic Health: A Narrative Review. Nutrients 17(3): 428.

Amararathna, M., Hoskin, D.W., and Rupasinghe, H.P.V. (2020). Anthocyanin-rich haskap (*Lonicera caerulea* L.) berry extracts reduce nitrosamine-induced DNA damage in human normal lung epithelial cells in vitro. Food Chem. Toxicol. 141: 111404.

Anbualakan, K., Tajul Urus, N.Q., Makpol, S., Jamil, A., Mohd Ramli, E.S., Md Pauzi, S.H., and Muhammad, N. (2022). A Scoping Review on the Effects of Carotenoids and Flavonoids on Skin Damage Due to Ultraviolet Radiation. Nutrients 15(1): 92.

Balić, A., and Mokos, M. (2019). Do We Utilize Our Knowledge of the Skin Protective Effects of Carotenoids Enough? Antioxidants (Basel) 8(8):

259.
Bernerd, F., Passeron, T., Castiel, I., and Marionnet, C. (2022). The Damaging Effects of Long UVA (UVA1) Rays: A Major Challenge to Preserve Skin Health and Integrity. Int. J. Mol. Sci. 23(15): 8243.
Budzianowska, A., Banaś, K., Budzianowski, J., and Kikowska, M. (2025). Antioxidants to Defend Healthy and Youthful Skin—Current Trends and Future Directions in Cosmetology. Appl. Sci. 15(5): 2571.
Bulama, I., Nasiru, S., Bello, A., Abbas, A.Y., Nasiru, J.I., Saidu, Y., Chiroma, M.S., Mohd Moklas, M.A., Mat Taib, C.N., Waziri, A., and Suleman, B.L. (2022). Antioxidant-based neuroprotective effect of dimethylsulfoxide against induced traumatic brain injury in a rats model. Front. Pharmacol. 13: 998179.
Calabrese, E.J., and Kozumbo, W.J. (2021). The phytoprotective agent sulforaphane prevents inflammatory degenerative diseases and age-related pathologies via Nrf2-mediated hormesis. Pharmacol. Res. 163: 105283.
Calniquer, G., Khanin, M., Ovadia, H., Linnewiel-Hermoni, K., Stepensky, D., Trachtenberg, A., Sedlov, T., Braverman, O., Levy, J., and Sharoni, Y. (2021). Combined Effects of Carotenoids and Polyphenols in Balancing the Response of Skin Cells to UV Irradiation. Molecules 26(7): 1931.
Chatgilialoglu, C., Ferreri, C., Krokidis, M.G., Masi, A., and Terzidis, M.A. (2021). On the relevance of hydroxyl radical to purine DNA damage. Free Radic. Res. 55: 384–404.
Chen, X., Deng, Z., Zheng, L., Zhang, B., Luo, T., and Li, H. (2021). Interaction between Flavonoids and Carotenoids on Ameliorating Oxidative Stress and Cellular Uptake in Different Cells. Foods 10(12): 3096.
de Almeida, A., de Oliveira, J., da Silva Pontes, L.V., de Souza Junior, J.F., Goncalves, T.A.F., Dantas, S.H., de Almeida Feitosa, M.S., Silva, A.O., and de Medeiros, I.A. (2022). ROS: Basic Concepts, Sources, Cellular Signaling, and its Implications in Aging Pathways. Oxid. Med. Cell. Longev. 2022: 1225578.
Eruslanov, E., and Kusmartsev, S. (2010). Identification of ROS using oxidized DCFDA and flow-cytometry. Methods Mol. Biol. 594: 57–72.
Groten, K., Marini, A., Grether-Beck, S., Jaenicke, T., Ibbotson, S.H., Moseley, H., Ferguson, J., and Krutmann, J. (2019). Tomato Phytonutrients Balance UV Response: Results from a Double-Blind, Randomized, Placebo-Controlled Study. Skin Pharmacol. Physiol. 32: 101–108.
Hegedűs, C., Juhasz, T., Fidrus, E., Janka, E.A., Juhasz, G., Boros, G., Paragh, G., Uray, K., Emri, G., Remenyik, E., and Bai, P. (2021). Cyclobutane pyrimidine dimers from UVB exposure induce a hypermetabolic state in keratinocytes via mitochondrial oxidative stress. Redox. Biol. 38: 101808.
Jesus, A., Mota, S., Torres, A., Cruz, M.T., Sousa, E., Almeida, I.F., and Cidade, H. (2023). Antioxidants in Sunscreens: Which and What For? Antioxidants (Basel) 12(1): 138.
Jomova, K., Alomar, S.Y., Alwasel, S.H., Nepovimova, E., Kuca, K., and Valko, M. (2024). Several lines of antioxidant defense against oxidative stress: antioxidant enzymes, nanomaterials with multiple enzyme-mimicking activities, and low-molecular-weight antioxidants. Arch. Toxicol. 98: 1323–1367.
Kciuk, M., Marciniak, B., Mojzych, M., and Kontek, R. (2020). Focus on UV-Induced DNA Damage and Repair-Disease Relevance and Protective Strategies. Int. J. Mol. Sci. 21(19): 7264.
Kobayashi, K., Suzauddula, M., Bender, R., Li, C., Li, Y., Sun, X.S., and Wang, W. (2025). Functional Properties and Potential Applications of Wheat Bran Extracts in Food and Cosmetics: A Review of Antioxidant, Enzyme-Inhibitory, and Anti-Aging Benefits. Foods 14(3): 515.
Kozlov, A.V., Javadov, S., and Sommer, N. (2024). Cellular ROS and Antioxidants: Physiological and Pathological Role. Antioxidants (Basel) 13(5): 602.
Lagunas-Rangel, F.A., and Bermudez-Cruz, R.M. (2020). Natural Compounds That Target DNA Repair Pathways and Their Therapeutic Potential to Counteract Cancer Cells. Front. Oncol. 10: 598174.
Lee, K.H., Do, H.K., Kim, D.Y., and Kim, W. (2021). Impact of chlorogenic acid on modulation of significant genes in dermal fibroblasts and epidermal keratinocytes. Biochem. Biophys. Res. Commun. 583: 22–28.
Manzoor, M.F., Zeng, X.A., Rahaman, A., Siddeeg, A., Aadil, R.M., Ahmed, Z., Li, J., and Niu, D. (2019). Combined impact of pulsed electric field and ultrasound on bioactive compounds and FT-IR analysis of almond extract. J. Food Sci. Technol. 56: 2355–2364.
Mapoung, S., Umsumarng, S., Semmarath, W., Arjsri, P., Srisawad, K., Thippraphan, P., Yodkeeree, S., and Dejkriengkraikul, P. (2021). Photoprotective Effects of a Hyperoside-Enriched Fraction Prepared from Houttuynia cordata Thunb. on Ultraviolet B-Induced Skin Aging in Human Fibroblasts through the MAPK Signaling Pathway. Plants (Basel) 10(12): 2628.
Mathew, S.T., Bergstrom, P., and Hammarsten, O. (2014). Repeated Nrf2 stimulation using sulforaphane protects fibroblasts from ionizing radiation. Toxicol. Appl. Pharmacol. 276: 188–194.
Moskwa, J., Bronikowska, M., Socha, K., and Markiewicz-Zukowska, R. (2023). Vegetable as a Source of Bioactive Compounds with Photoprotective Properties: Implication in the Aging Process. Nutrients 15(16): 3594.
Murugesan, K., Mulugeta, K., Hailu, E., Tamene, W., and Alagar Yadav, S. (2021). Insights for integrative medicinal potentials of Ethiopian Kale (*Brassica carinata*): Investigation of antibacterial, antioxidant potential and phytocompounds composition of its leaves. Chin. Herb. Med. 13: 250–254.
Noda, M., Ma, Y., Yoshikawa, Y., Imanaka, T., Mori, T., Furuta, M., Tsuruyama, T., and Yoshikawa, K. (2017). A single-molecule assessment of the protective effect of DMSO against DNA double-strand breaks induced by photo-and gamma-ray-irradiation, and freezing. Sci. Rep. 7: 8557.
Ortega-Hernandez, E., Antunes-Ricardo, M., and Jacobo-Velazquez, D.A. (2021). Improving the Health-Benefits of Kales (*Brassica oleracea* L. var. . Plants (Basel) 10(12): 2629.
Oyerinde, A.S., Selvaraju, V., Boersma, M., Babu, J.R., and Geetha, T. (2025). Effect of H_2O_2 induced oxidative stress on volatile organic compounds in differentiated 3T3-L1 cells. Sci. Rep. 15: 2597.
Quijano-Ortega, N., Fuenmayor, C.A., Zuluaga-Dominguez, C., Diaz-Moreno, C., Ortiz-Grisales, S., García-Mahecha, M., and Grassi, S. (2020). FTIR-ATR Spectroscopy Combined with Multivariate Regression Modeling as a Preliminary Approach for Carotenoids Determination in Cucurbita spp. Appl. Sci. 10(11): 3722.
Rajnochová Svobodová, A., Rysava, A., Cizkova, K., Roubalova, L., Ulrichova, J., Vrba, J., Zalesak, B., and Vostalova, J. (2022). Effect of the flavonoids quercetin and taxifolin on UVA-induced damage to human primary skin keratinocytes and fibroblasts. Photochem. Photobiol. Sci. 21: 59–75.
Rock, C.L., Thomson, C., Gansler, T., Gapstur, S.M., McCullough, M.L., Patel, A.V., Andrews, K.S., Bandera, E.V., Spees, C.K., Robien, K., Hartman, S., Sullivan, K., Grant, B.L., Hamilton, K.K., Kushi, L.H., Caan, B.J., Kibbe, D., Black, J.D., Wiedt, T.L., McMahon, C., Sloan, K., and Doyle, C. (2020). American Cancer Society guideline for diet and physical activity for cancer prevention. CA Cancer J. Clin. 70: 245–271.
Sangweni, N.F., Dludla, P.V., Chellan, N., Mabasa, L., Sharma, J.R., and Johnson, R. (2021). The Implication of Low Dose Dimethyl Sulfoxide on Mitochondrial Function and Oxidative Damage in Cultured Cardiac and Cancer Cells. Molecules 26(23): 7305.
Sies, H., and Jones, D.P. (2020). Reactive oxygen species (ROS) as pleiotropic physiological signalling agents. Nat. Rev. Mol. Cell Biol. 21: 363–383.
Stefanowicz-Hajduk, J., and Ochocka, J.R. (2020). Real-time cell analysis system in cytotoxicity applications: Usefulness and comparison with tetrazolium salt assays. Toxicol. Rep. 7: 335–344.
Suraweera, T.L., Rupasinghe, H.P.V., Dellaire, G., and Xu, Z. (2020). Regulation of Nrf2/ARE Pathway by Dietary Flavonoids: A Friend or Foe for Cancer Management? Antioxidants (Basel) 9(10): 973.
Tang, X., Yang, T., Yu, D., Xiong, H., and Zhang, S. (2024). Current insights and future perspectives of ultraviolet radiation (UV) exposure: Friends and foes to the skin and beyond the skin. Environ. Int. 185: 108535.
Tomas, M., Günal-Köroğlu, D., Kamiloglu, S., Ozdal, T., and Capanoglu, E. (2025). The state of the art in anti-aging: plant-based phytochemicals for skin care. Immun. Ageing. 22: 5.
Tong, L., and Wu, S. (2018). The Mechanisms of Carnosol in Chemoprevention of Ultraviolet B-Light-Induced Non-Melanoma Skin Cancer Formation. Sci. Rep. 8: 3574.
Valisakkagari, H., and Rupasinghe, H.P.V. (2025). Application of Response Surface Methodology for the Extraction of Phytochemicals from Upcycled Kale (*Brassica oleracea* var. acephala). Nutraceuticals

5(1): 2.
Valisakkagari, H., Chaturvedi, C., and Rupasinghe, H.P.V. (2024). Green Extraction of Phytochemicals from Fresh Vegetable Waste and Their Potential Application as Cosmeceuticals for Skin Health. Processes 12(4): 742.
Wang, L., Kim, H.S., Oh, J.Y., Je, J.G., Jeon, Y.J., and Ryu, B. (2020). Protective effect of diphlorethohydroxycarmalol isolated from Ishige okamurae against UVB-induced damage in vitro in human dermal fibroblasts and in vivo in zebrafish. Food Chem. Toxicol. 136: 110963.
Xue, N., Liu, Y., Jin, J., Ji, M., and Chen, X. (2022). Chlorogenic Acid Prevents UVA-Induced Skin Photoaging through Regulating Collagen Metabolism and Apoptosis in Human Dermal Fibroblasts. Int. J. Mol. Sci. 23(13): 6941.
Zheng, K., Ma, J., Wang, Y., He, Z., and Deng, K. (2020). Sulforaphane Inhibits Autophagy and Induces Exosome-Mediated Paracrine Senescence via Regulating mTOR/TFE3. Mol. Nutr. Food Res. 64(14): 1901231.